Available online at www.sciencedirect.com

ScienceDirect

Transportation Research Procedia 00 (2018) 000–000

Transportation Research Procedia

www.elsevier.com/locate/procedia

World Conference on Transport Research - WCTR 2019 Mumbai 26-31 May 2019

A Model Analysis of the Saturation Flow Rate Influenced by Downstream Conditions

Hong Zhu [a]*, Hideki Nakamura [a]

[a] *Graduate School of Environmental Studies, Nagoya University, C1-2(651), Furo-cho, Chikusa-ku, Nagoya 464-8603, Japan.*

Abstract

Saturation flow rate (SFR, hereinafter) serves as the most important parameter in the analysis of a signalized intersection, which plays a main role in estimating capacity and signal timing. In the area where intersections are closely spaced and traffic demand is high, drivers' desire for quick speed up is demotivated by several negative downstream conditions, such as limited available storage length, long queue, or poorly coordinated traffic signals, which leads to the low SFR of upstream lane groups. After comparing the pros and cons of previous studies, this paper proposes an improved intelligent driver model (IDM, hereinafter) for reproducing these phenomena and calibrate parameters with the genetic algorithm based on observed driver behaviors. Through scenario simulation, it is proved that the new model can reproduce the SFR reduction under different downstream conditions. As the queue in the downstream segment at the onset of green becomes longer and the offset between the downstream intersection and upstream intersection becomes larger, the SFR at the upstream intersection approach tends to deteriorate. By comparing with empirical data the model is further tested and the result proved that it can estimate the influenced SFR well.

Peer-review under responsibility of WORLD CONFERENCE ON TRANSPORT RESEARCH SOCIETY.

Keywords: Signalized intersection, Saturation flow rate, Downstream conditions, Car following model;

1. Introduction

Signalized intersection is the fundamental component of the urban transportation system and intersection-related congestion is becoming more frequent, which has attracted a considerable attention in recent years. On the other hand, longer spaces are required to accommodate a departing flow with higher traffic demands in the downstream segment. However, the presence of long queues in the downstream segment will diminish the performance of the subject intersection approach. This phenomenon can be frequently observed in large urban areas where the traffic volume is heavy, intersection spacing is short and cycle length is long.

At any typical signalized intersection, vehicles would arrive during the red time and wait in the queue, as the signal display turns green, the platoons will reach the maximal departure flow rate after a few seconds, which is generally regarded as Saturation Flow Rate (SFR, hereinafter). In Highway Capacity Manual (HCM, hereinafter) 6th Edition (2016), SFR is defined as, the equivalent hourly rate at which previously queued vehicles can traverse an intersection approach under prevailing conditions, assuming that the green signal is available at all times and no lost times are experienced. It is important in transportation engineering because it serves as the basis for setting traffic signal timings, estimating the capacity of signalized intersections and evaluating the mobility performance.

If the queue in the downstream segment is still waiting for the traffic signal to turn green or the space available behind the queue in the downstream segment is small the drivers departing from subject intersection approach would be discouraged to accelerate

* Corresponding author. Tel.: +81-52-789-3832; fax: +81-52-789-3837.
E-mail address: zhu.hong@a.mbox.nagoya-u.ac.jp

Peer-review under responsibility of WORLD CONFERENCE ON TRANSPORT RESEARCH SOCIETY

to discharge. It is expected that the longer the downstream queue is, the greater such an impact. Thus, the SFR at the subject intersection approach is expected to be affected by the downstream conditions. Also, the sustained spillback is one of the downstream impacts that vehicles of upstream intersection cannot pass the stop line because of the extension of the downstream queue. This phenomenon will significantly reduce the efficiency of the upstream intersection. It has been referred in HCM 6th Edition and added into the estimation model as a reduction parameter. However, through observation, it is easy to know that when they are facing with the downstream queue, most of the drivers will choose a lower speed than free start in order to have a more comfortable and safer trip. Even without spillback from the downstream segment, the upstream flow could also be influenced by the presence of downstream queue. Therefore, sustained spillback is an extreme case which is not all-inclusive for the downstream impacts. However, the existing estimation methods for SFR does not fully consider the downstream influence and they could overestimate the real value. Therefore, this study mainly focuses on the SFR reduction before spillback happens.

The objective of this study is to propose a new estimating model for the influenced SFR considering downstream impacts by improving the IDM and discuss the influence of each downstream parameter on SFR. The terminologies referred in this paper are listed and explained in the following nomenclature table.

Nomenclature

s	adjusted saturation flow rate (veh/h/ln)
s_0	base saturation flow rate (pcu/h/ln)
f_w	adjustment factor for lane width
f_{HVg}	adjustment factor for heavy vehicles and grade
f_p	adjustment factor for the existence of a parking lane and parking activity adjacent to lane group
f_{bb}	adjustment factor for blocking effect of local buses that stop within intersection area
f_a	adjustment factor for area type
f_{LU}	adjustment factor for lane utilization
f_{LT}	adjustment factor for right-turn vehicle presence in a lane group
f_{RT}	adjustment factor for right-turn vehicle presence in a lane group
f_{Lpb}	pedestrian adjustment factor for left-turn groups
f_{Rpb}	pedestrian-bicycle adjustment factor for right-turn groups
f_{wz}	adjustment factor for work-zone presence at the intersection
f_{ms}	adjustment factor for downstream lane blockage
f_{sp}	adjustment factor for sustained spillback
a^t	acceleration at time t (m/s^2)
$f_{car\text{-}follow}$	car-following module (m/s^2)
$f_{downstream}$	downstream influence module (m/s^2)
h_d	distance headway or space headway (m)
l	vehicle length (m)
τ	drivers reaction time (s)
d_b	brake distance, the product of the reaction time and the current speed (m)
ω	distance from upstream 1st vehicle's front bumper to stop line (m)
d_0	minimum stopping distance (m)
n	number of vehicles in downstream queue
l_s	segment length the distance from upstream stop line to the downstream stop line (m)
l_q	length of downstream the queue (m)
l_{as}	distance from the front bumper of the upstream 1st vehicle to the rear bumper of the downstream last vehicle (m)
$offset$	time difference between the downstream and subject intersection green indication (s)
v_{op}	optimal speed (m/s)
v_0	velocity the vehicle would drive at in free traffic (m/s)
T	minimum time headway (s)
a	maximum vehicle acceleration (m/s^2)
b	comfortable braking deceleration (m/s^2)
δ	acceleration exponent which is usually set to 4
d_α	net distance (m)
d^*	desired minimum net distance (m)
β	downstream module
c	extent of the downstream impact
k	exponent of downstream impact
s_i^{data}	empirical trajectory data on time series of vehicle i
s_i^{sim}	simulated trajectory data on time series of vehicle i with the observed leading vehicle serving as externally input
m	number of vehicles for fitness calculation

SFR_{obs}	SFR for cycle i (veh/h/ln)
h_{si}	average saturation headway for cycle i (s)
T_{ni}	discharge time of n^{th} queued vehicle during cycle i (s)
T_{4i}	discharge time of 4th queued vehicle during cycle i (s)
n_i	number of queued vehicles observed during cycle i

2. Literature Review

HCM 6th Edition explains the procedure to calculate the SFR by using the following equation:

$$s = s_0 f_w f_{HVg} f_p f_{bb} f_a f_{LU} f_{LT} f_{RT} f_{Lpb} f_{Rpb} f_{wz} f_{ms} f_{sp} \quad (1)$$

Among all the adjustment factors, the adjustment factor for downstream mid segment lane blockage (f_{ms}) and that for sustained spillback (f_{sp}) represent the adjustment for the downstream conditions. f_{ms} considers the effect of lane blockage only due to construction work or due to the occurrence of a special event, like an accident, etc. Whereas, f_{sp} considers the effect of downstream conditions as a result of sustained spillback which is the result of oversaturation (i.e. more vehicles discharging from the subject intersection than which can be served at the downstream intersection).

Akcelik and Rouphail (1992) were the first to study non-isolated signalized intersections. By a simple queue interaction analytical model, they revealed that the presence of downstream queues has a strong influence on the performance of the paired intersection system, even when the system operates below the capacity. Finally, they recommended analyzing the reduction in the SFR due to the influence of downstream queue availability.

Ahmed and Abu-Lebdeh (2005) developed a macroscopic model for a hypothetical two-signal system to estimate the delay at signalized intersections caused by the downstream congestion by means of basic traffic flow properties and control parameters at neighboring signalized intersections. They found that delay caused by the downstream conditions is significant, therefore must be included in level-of-service and capacity analysis. Their study also resulted in finding that offsets and green splits at upstream and downstream intersections play key roles in reducing delay.

The Traffic Signal Timing Manual (2008) recommended that the performance measures of intersection treatment should include queue lengths, and the objectives are to minimize the time period during which queue spillback occurs and to manage queue interactions between intersections during oversaturated conditions.

Hashemi et al. (2017) analyzed the traffic flow in two corridors with closely spaced intersections in Japan and proposed Normal and Weibull distribution models for the influenced SFR. However, the accuracy of the distribution model highly depends on the data quantity. Extension and application are limited. As a result, the proposed model can only be applied to evaluate the downstream impacts but cannot estimate the SFR value under different downstream conditions.

After attempting several available analytical models, Yu and Sulijoadikusumo (2012) suggested that currently available models for representing downstream disturbance are either data intensive and require network-wide simulation models or mathematical programming models. It is hard to find enough cases in real life to cover all scenarios, thus, a mathematical model with small data requirements is necessary.

3. Methodology

3.1. Model structure statement

By observation, it is found that the distance between the upstream discharging platoon and downstream queueing vehicles is short enough for upstream drivers to know actions of downstream vehicles. Under these circumstances, the upstream discharging vehicle should not be treated as a free-start vehicle but the follower of the downstream platoon.

Subsequently, as an attempt, several common car-following models have been tested to simulate upstream vehicles' trajectories (time-space diagram) depending on actions of queueing vehicles in the downstream segment. However, further analysis found that the existing car-following models do not fit the real data quite well. The simulated trajectories are either approaching the downstream platoon too quickly (e.g. GM Model) or directly accelerating to the desired speed in a small available space (e.g. IDM) which is not reasonable for human drivers. One of the reasons is that most of the current car-following models are designed for modelling the uninterrupted-flow on freeways or expressways, less attention has been paid to the interrupted flow on the urban roads, which is also recognized by Cohen (2002).

In reality, when drivers are facing with downstream queues, they will not only react to front vehicles but also anticipate the action of the downstream platoon based on the information such as offset, downstream queue length, etc. Hence, in this study, the IDM is improved by adding downstream influence module and the basic structure of the new model is as follows.

$$a^t = f_{car-follow} + f_{downstream} \quad (2)$$

3.2. Concept and definition regarding the downstream influence

Considering that the downstream constraints which drivers can perceive are time-space two dimensional, a virtual speed value v_{op} is introduced to discuss downstream impacts. Generally, while discharging vehicles could not avoid joining the downstream queue, optimaizing their speed and acceleration to pursue the most comfortable and efficient driving process is the subconscious of most drivers. For easy understanding the following statement, real trajectories are deformed by the following 2 steps firstly, as Fig. 1 shows.

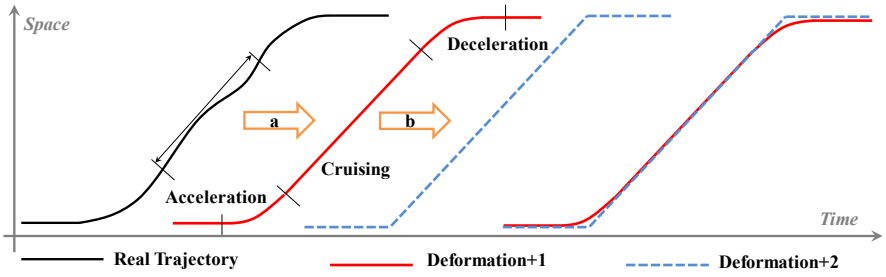

a. assuming that after acceleration, vehicles will keep cruising at an unchanged speed until they have to stop.
b. neglecting the acceleration and deceleration part.

Fig. 1. Trajectory Deformation

When drivers are waiting at upstream approaches, they can receive a lot of downstream information such as downstream queue length, available space, segment length, and signal display. The driving strategy of passing the downstream link can be made based on the information. Among them, joining the downstream queue just at the time when the last vehicle starts to move is the best one because it can guarantee smaller speed changes but not increase the travel time. The cruising speed in this optimal strategy is called as optimal speed, v_{op}. The derivation process of v_{op} is shown in the Fig. 2 and the following formulas.

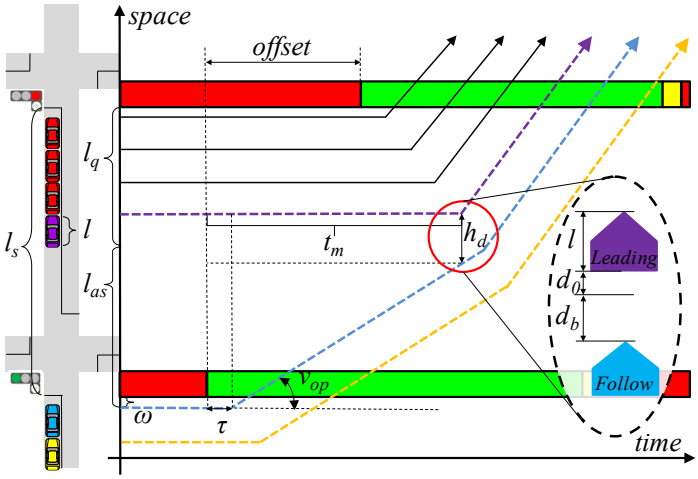

Fig. 2. Deduction of v_{op}

$$v_{op}=\frac{l_{as}+l-h_d}{t_m-\tau} \tag{3}$$

Substitute h_d into formula (3), then

$$v_{op}=\frac{l_{as}-d_0}{t_m} \tag{4}$$

Also, it can be inferred that

$$l_{as}=l_s-l_q+\omega \tag{5}$$

$$l_q = nl + (n-1)d_0 + \omega \tag{6}$$

$$t_m = n\tau + offset \tag{7}$$

By substituting the formula (5), (6) and (7) into (8), the relations between *offset*, l_s, l_{as}, and v_{op} can be deduced.

$$v_{op} = \begin{cases} \dfrac{l_s - l_q}{\tau \dfrac{l_q + d_0}{d_0 + l} + offset} & , \ if \ \dfrac{l_s - l_q}{\tau \dfrac{l_q + d_0}{d_0 + l} + offset} \geq 0 \\ +\infty & , \ otherwise \end{cases} \tag{8}$$

It is easy to imagine that when the desired speed v_0 is larger than v_{op}, the driver's desire for free driving will be demotivated in time and space. With the increase of the difference between v_0 and v_{op}, the adverse effect will gradually increase. When the v_{op} is larger than v_0, the vehicle can pass through the downstream segment at the v_o, which means that downstream conditions have no negative effects on the upstream platoon. According to the above statement and treat v_{op} as a core indicators, a new model is proposed by improving the intelligent driver model. IDM is selected because it is one of the most robust existing car-following models. The dynamics of vehicle α are described by the following two ordinary differential equations.

$$\begin{cases} \dfrac{dx_\alpha}{dt} = v_\alpha \\ \dfrac{dv_\alpha}{dt} = a\left(1 - \left(\dfrac{v_\alpha}{v_0}\right)^\delta - \left(\dfrac{d^*(v_\alpha, \Delta v_\alpha)}{d_\alpha}\right)^2\right) - \beta(c, k, v_{op}, v_0) \end{cases} \tag{9}$$

$$d^*(v_\alpha, \Delta v_\alpha) = d_0 + v_\alpha T + \frac{v_\alpha \Delta v_\alpha}{2\sqrt{ab}} \tag{10}$$

$$\beta(c, k, v_{op}, v_0) = \begin{cases} c\left(\dfrac{v_0 - v_{op}}{v_0}\right)^k & , \ v_{op} < v_0 \\ 0 & , \ v_{op} \geq v_0 \end{cases} \tag{11}$$

In order to maintain the car-following function, the first half part of the model preserves the original formula of IDM, which is proposed by Treiber, et al. (2000). For vehicle α, α - 1 refers to the vehicle directly in front of vehicle α. x_α gives its position at time t and v_α gives its velocity. l_α denotes the vehicle length and the net distance headway is defined as $d_\alpha = x_{\alpha-1} - x_\alpha - l_{\alpha-1}$. Furthermore, in order to simplify the process, no heavy vehicles are considered in this research and all passenger vehicles are assumed to be of the same length l. In addition, the velocity difference or approaching rate is $\Delta v_\alpha = v_\alpha - v_{\alpha-1}$. The second module is designed to measure the downstream impact. Among these parameters, c (m/s^2) represents the extent of the downstream impact and k is the adjustment factor for determining its increasing type.

3.3. Characteristics of the downstream influence module

For testing the characteristics of the downstream influence module β, v_0, c, k, d_0, τ, and l are assumed to be 20m/s, 1.5m/s^2, 4, 2m, 0.5s, and 4.5m, respectively. Two scenarios l_s=200m and l_s=150m are set. In each scenario, the *offset* decreases from 10s to -10s and the queue length l_q increases from 0m to 200m or 150m. The testing results are as follows. In Fig. 3(a), as the l_q increases, the l_{as} decreases and the *offset* increases from -10s to 10s, the value of β becomes larger, which is consistent with the reality that positive offset, long queue, and limited available space will demotivate drivers' desire for quickly running. Comparing with Fig. 3(a) and (b), the same queue length in (b) will get a higher β, which is consistent with the reality that longer segment length could accommodate longer queue and mitigate the downstream influence.

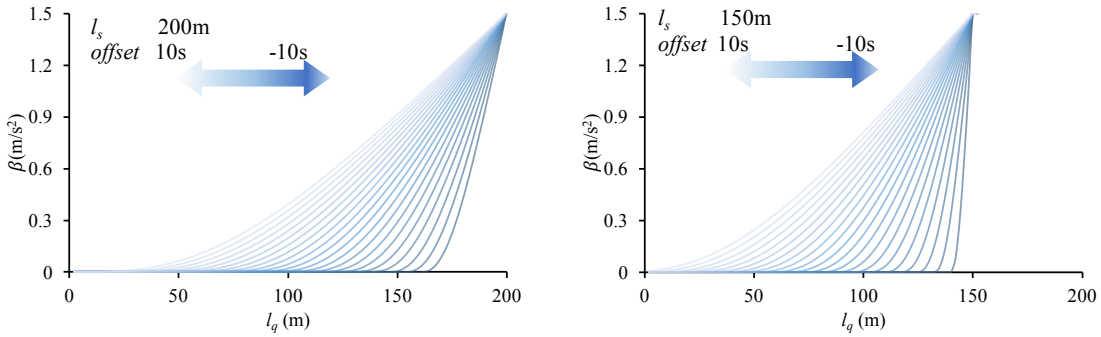

(a) l_s=200m (b)) l_s=150m

Fig. 3. Characteristics of the downstream influence module

4. Parameter Calibration

4.1. Calibration method

Simulation performance is the main point for evaluating a car-following model, which determines its adaptability. For a certain traffic flow, if the car-following model can accurately reproduce the most vehicles' trajectory and maintain a small error with empirical data, it could be said that this model has a good fit for this traffic flow and it can be applied to further discuss macroscopic quantities just like the work in traffic simulation software. In this study, in order to capture drivers' average behavior, the fitness formula is designed considering the mix error measure mentioned in Kesting and Treiber (2008) as shown in equation (12).

$$Fitness = \frac{1}{m}\sum_{i}^{m}\sqrt{\frac{1}{\left\langle s_i^{data}\right\rangle}\times\left\langle\frac{\left(s_i^{sim}-s_i^{data}\right)^2}{\left|s_i^{data}\right|}\right\rangle} \tag{12}$$

Here, the expression $\langle . \rangle$ means the temporal average of time series of duration ΔT that is,

$$\langle z\rangle=\frac{1}{\Delta T}\int_0^{\Delta T} z(t)\,dt \tag{13}$$

The optimization process is achieved by an intelligent optimization method, the genetic algorithm. The optimization process is as follows:

- Firstly, a population set is generated stochastically within the constraints. A population consists of N individuals and each individual represents a parameter setting (gene, hereinafter) of a car-following model;
- In each generation, fitness scores of all individuals in the population are calculated via the objective equation (12);
- The best individual will be kept unchanged. Pairs of two individuals are selected from the other individuals randomly based on fitness values and make crossover to generate a new individual. Also, the genes of all individuals except the best individual are varied randomly, which is corresponding to the mutation process and it is controlled by a given probability. Then, the new generation will be used in the next iteration.
- Two termination criterions are implemented. If the generations reach a fixed number or fitness values become convergence, iteration stops and output the final result.

IDM contains 5 parameters and the improved IDM (IDM+, hereinafter) not only covers these 5 indicators but also includes other 2 new indicators. According to the meaning of the index, the overlap part of IDM and IDM+ will be calibrated by same values. To restrict the parameter space to reasonable and positive parameter values without excluding possible solutions, the constraints in Table 1 are applied for the minimum and maximum values.

Table 1. Parameters constraints.

Parameters	Constraints [min, max]
IDM	
v_0	[1,30] m/s
T	[0,1.5] s
a	[0.1,6] m/s^2
b	[0.1,4] m/s^2
s_0	[0.1,8] m
IDM+	
c	[0,6] m/s^2
k	[0.1,6]

4.2. Empirical data

In this study, the empirical data is collected from Yasukuni-Dori, a corridor with closely spaced intersections in Tokyo, Japan. There are 5 approaches located on this road. They are Jimbocho westbound (WB) approach, Jimbocho eastbound (EB) approach, Sendaimae WB approach, Sendaimae EB approach, and Matsubara EB approach separately. A video survey was conducted on Tuesday, January 31 and Wednesday, February 1, 2017, with sunny weather by including five approaches of three different intersections along the same corridor. Around 235 cycles were recorded for each approach, covering both morning and evening peak hours for the major through EB and WB approaches. The distance between the intersections ranges between 116 m to 248 m. Each approach consists of an exclusive right turning, two through and a shared through and left turning lanes. On this road traffic signals are all actuated depending on the real-time traffic. Therefore, green time intervals and offsets between two neighboring intersections were slightly changing by cycles without break their coordination. Site description is provided in Fig. 4.

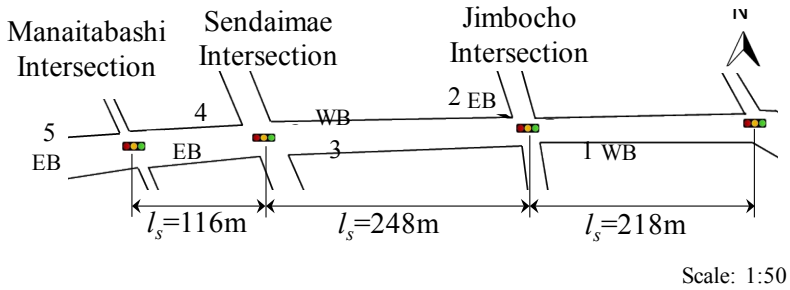

Fig. 4. Site description

Starting from the onset of upstream green until the vehicle joining the downstream queue or passing the downstream stop line, vehicles' position points are recorded by an image processing software developed by Suzuki and Nakamura (2006). A total of 30 sets were collected and every set of data contains trajectory records of vehicle 1-7 (the vehicle number is defined in the next section). In addition, in order to guarantee the universality of the experiment, heavy vehicle and abnormal behaviors (extremely fast or slow, lane changing) are excluded. Fig.5 shows an example of recorded vehicle trajectories.

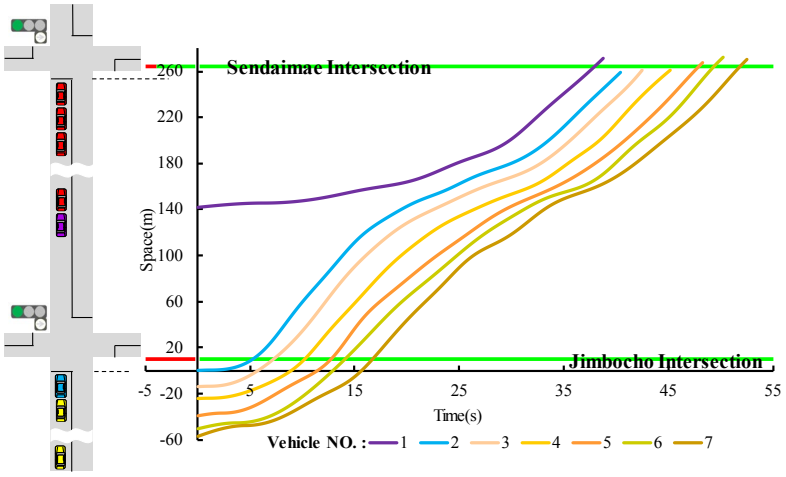

Fig. 5. Data example

4.3. Number of influenced vehicles

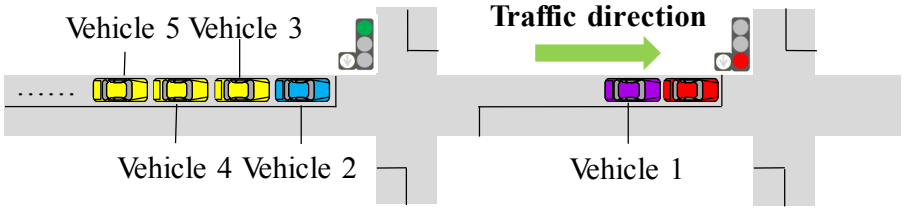

Fig. 6. Vehicle numbers

For convenience, vehicles in the system are numbered as Fig. 6 shows. The last vehicle in the downstream queue is numbered as vehicle 1 and the upstream leading vehicle is numbered as vehicle 2, etc. Firstly, with the observed trajectories of vehicle 1 serving as input data, the simulated trajectories of vehicles 2 can be solved. By substituting the observed data of vehicle 2, the simulated trajectory of vehicle 3 can be deduced. Then, the simulated trajectories of vehicles 4, 5, 6, and 7 can also be calculated successively by inputting empirical trajectory of their corresponding front car by analogy. All the simulation results from the 2-7 vehicles are included in the simulated data set.

In an upstream platoon, obviously, visions of vehicles differ by position in the platoon. First few vehicles could know downstream queue length, available space and offset clearly. On the other hands, drivers in the rear section of the platoon can not see downstream queue very well, because a large portion of drivers' vision is obscured by front vehicles. Whereas, they are still able to observe signal indicates due to high angles of signal lamps. It means that as the position in the platoon increases, the amount of received downstream information decreases and downstream impacts gradually reduce. Thus during calibration, the relationship between downstream influence and vehicle position is also discussed.

4.4. Calibration result

As a result, the optimal parameter calibration is solved by applying the optimization method and calibration process mentioned above. The model calibration result is shown in Table 2. Because the genetic algorithm always gives the best calibration, the difference in parameter *c* can reflect the extent of downstream impacts. In Table. 2, the value of *c* maintains a slightly decreasing trend on vehicle number, which proves the previous assumption. Also, almost for the vehicles in every position IDM+ get lower fitness values than IDM except the vehicle 6. Regarding the vehicle 6, the fitness value of IDM is 21.51% and that of IDM+ is 22.01% so that the difference between them is not obvious. Generally, the newly designed model has a better fit for the demotivated vehicle trajectories than the IDM and it reveals that downstream impacts do exist.

In addition, the low fitness values of vehicles 2, 3 and 4 also indicates that the downstream impact on upstream first three vehicles is more significant. However, this conclusion is only limited to the above survey site because different geometric designs lead to different fields of vision and the number of vehicles which are able to clearly know downstream conditions is different. For example, in a downhill section, drivers can see further than an uphill section. This topic deserves to be further discussed in the near future. Finally, the IDM+ calibrated by all vehicle trajectories will be adopted for the following analysis.

Table 2. Calibration result

	Fitness (%)		v_0 (m/s)		T (s)		a (m/s^2)		b (m/s^2)		s_0 (m)		c (m/s^2)	k
No.	**IDM+**	**IDM**	**IDM+**	**IDM**	**IDM+**	**IDM**	**IDM+**	**IDM**	**IDM+**	**IDM**	**IDM+**	**IDM**	**IDM+**	**IDM+**
2	13.27	28.27	19.81	13.22	1.62	1.42	2.12	2.14	3.98	3.81	1.98	2.04	1.74	1.72
3	12.29	27.32	18.29	15.11	1.67	1.15	2.18	2.01	4.12	3.71	2.02	1.94	1.71	1.92
4	14.12	24.88	17.31	19.12	1.57	1.68	2.16	1.92	3.82	3.93	2.23	2.12	1.53	1.82
5	21.99	26.57	15.21	16.31	1.33	1.03	2.54	2.01	3.67	3.89	1.93	2.07	1.34	1.77
6	22.01	21.51	12.44	13.56	1.28	1.84	2.15	2.12	3.84	3.61	2.36	1.87	1.36	1.91
7	22.12	22.51	18.48	14.52	1.23	1.35	2.21	1.99	3.57	3.74	2.31	1.94	1.4	1.78
All	17.28	25.27	17.82	14.82	1.12	1.52	2.14	2.05	3.98	3.91	2.05	2.05	1.42	1.83

5. Model Validation

5.1. Scenario simulation

The model calibrated by vehicles in all positions is adopted for the scenario simulation. Countless scenarios can be designed to simulate different downstream conditions and the following analysis are carried out on a hypothetical road section. Two intersections are connected by a bi-directional two-lane road. No heavy vehicle and moving vehicle between downstream queue and upstream platoon are considered. Furthermore, the traffic flow discharging from downstream intersection will not be influenced by its downstream conditions. The queue length, segment length, and offset are variables in this system.

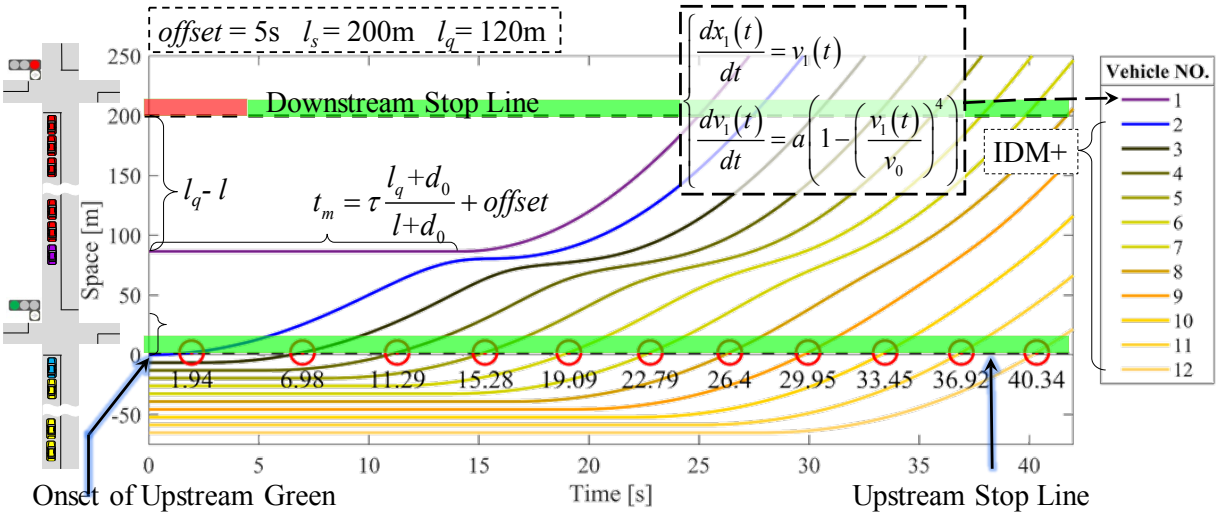

Fig. 7. Trajectory generated and simulation process in MATLAB

After setting these values, the trajectory of vehicle 1 can be modeled as a free start by assuming that the downstream intersection will no longer be influenced by the second downstream intersection, as Fig. 7 shows. Successively, the trajectories of vehicle 2, vehicle 3,… can be generated and the performance of discharge flow such as SFR can be measured and evaluated. In the next section, two scenarios of "l_s=200m" and "l_s=300m" are designed and discussed. For the "l_s=200m", the *offset* increases for -5s to 5s and l_q increases from 0m to 200m. For the "l_s=300m", the *offset* increases from -5s to 5s and l_q increases from 0m to 300m. At the onset of upstream green 12 queued vehicles discharge from upstream stopline without considering random arrival vehicles and all vehicle lengths are set to be 4.5m. The passing time on upstream stopline is recorded. Also, if any of these 12 cars are stopped by the extension of the downstream queue before the upstream stopline it would be counted as a spillback phenomenon and excluded. In order to ensure that the simulation is consistent with the reality, two detailed settings are designed in the program. Firstly, for the trajectory generated by improved IDM, collision is always unavoidable, which will reduce the simulation accuracy. In order to avoid this happens, an emergency braking link was set up in the simulation. When the $d_\alpha \leq 0.5 \times v_\alpha \tau$, the simulated vehicle will decelerate with 5m/s^2. This setting prevents the IDM+ model from asymptotic and local stability problem. On the other hand, regarding the reduction from downstream traffic, an impossible phenomenon that vehicle speed is less than zero may happen. Hence, a condition judgment module is adopted in the model. When the v_α<0, the simulated vehicle will not reverse but stop. The simulation process is implemented by the MATLAB software, one of the simulation results is shown in Fig. 7.

5.2. Simulation result

As shown in Fig. 7, simulated departure headways decrease sequentially as it stated in the theory and the saturated headways reach after a few vehicles. The SFRs can be deduced by letting 3600 divided by the saturated headways. The results of scenario simulation are shown in Fig. 8, Fig. 9, and Fig. 10.

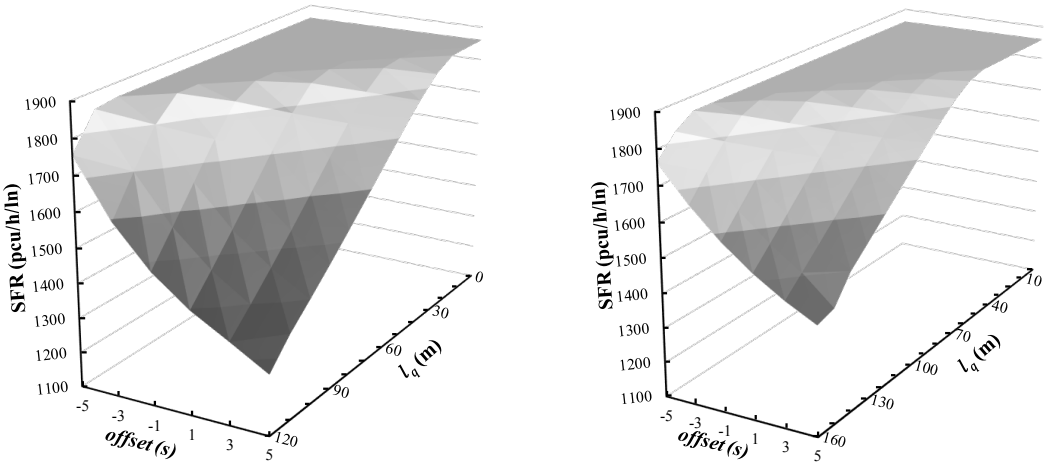

(a) l_s=200m (b) l_s=300m

Fig. 8. The relationship between SFR, l_q, and *offset*.

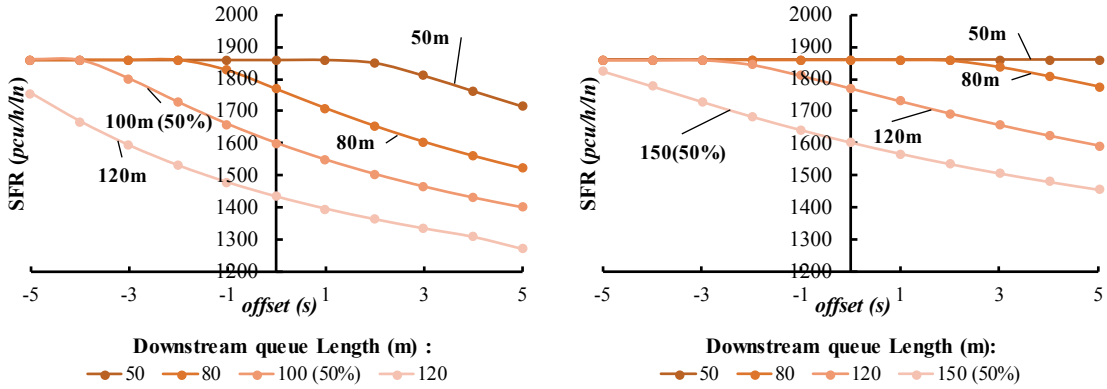

(a) l_s=200m (b) l_s=300m

Fig. 9. The relationship between SFR and *offset*.

In Fig. 8, these trend lines reveal that with increases in the l_q, and the *offset*, the SFR becomes lower because the long queue limits vehicle's available driving space and positive offset (red signal in the downstream queue) does not only increase the duration of the queue but also further demotivate drivers' desire for quickly running. On the contrary, as l_q and *offset* decrease, the SFR becomes higher and gradually approaches to a limit value which is approximately equal to 1900pch/h/ln. It can be inferred that the downstream reduction in this interval is almost 0. In addition, it is obvious that the decreasing trend in Fig. 8(a) is more intense than it in Fig. 8(b), because the short segment length is more sensitive to the downstream queue.

In Fig. 9(a) as the *offset* increases, the SFR decreases. When the downstream queue length is 50 meters, the value of SFR keeps steady between "*offset*=-5s" and "*offset*=2s", then decreases after "*offset*=2s". Whereas, when the downstream queue length is 80 meters, the value of SFR keeps steady only between "*offset*=-5s" and "*offset* =-2s", then drops after "*offset* =-2s". It indicates that the long queue will result in a drastic reduction in SFR but a short queue could mitigate the offset influence. Furthermore, the decreasing trend in Fig. 9(b) is milder than Fig. 9(a), which confirms that a longer segment length could accommodate longer queue again. On the other hand, while comparing the line of 100 (50%) in Fig. 9(a) and the line of 150 (50%) in Fig. 9(b), the decreasing trends are almost the same. Both of them represent that 50% of the downstream segment is occupied by queued vehicles and it can be inferred that the downstream density can give a better and more general explanation for measuring the downstream impact.

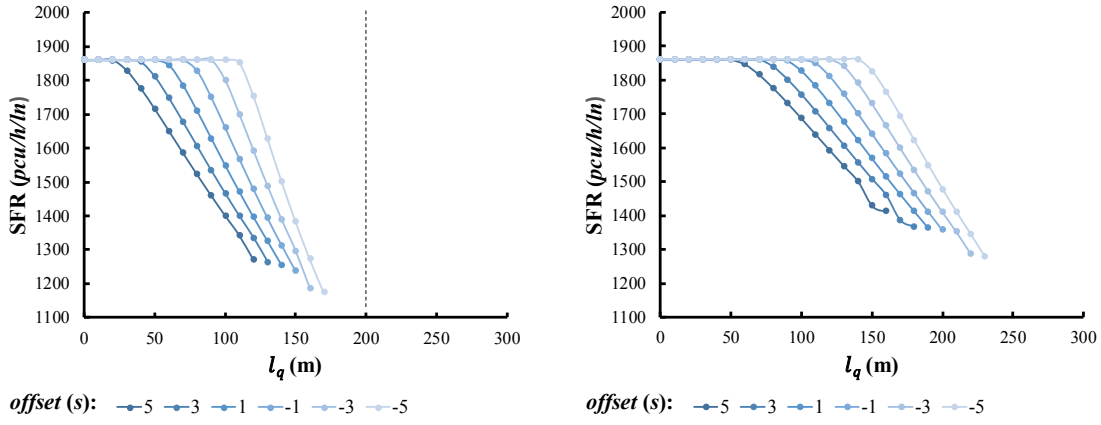

(a) l_s=200m (b) l_s=300m

Fig. 10. The relationship between SFR and l_q.

When observing the experimental results from the perspective of downstream queue length, it is found that as the l_q increases, the SFR decreases. The decreasing type of different *offset* is different. For example, when the *offset* is -5s, the value of SFR keeps steady until "l_q=120m", then decreases. However, when the *offset* is 5s, the value of SFR starts to decrease when "l_q=20m". It is also because the positive *offset* increases the duration of the downstream queue while a negative *offset* reduces its duration.

Moreover, in Fig. 10(a) none of the 6 trend lines extends to l_q=200m, some of the data points after $l_q \geqslant$120m are excluded due to spillback. It is found that the higher the *offset* is, the more data points are dropped. It also indicates that high positive offset values are more likely to trigger spillback which could seriously harm traffic efficiency. In addition, compared to Fig. 10(a), slopes of the curves in Fig. 10(b) are smaller. The same downstream queue length on a longrt road segment has a less negative effect on upstream discharge flow. It is also because longer segment length provide upstream vehicles more available space and alleviates the downstream impact.

5.3. Comparison with empirical data

At last, model's validity is further verified by comparing with empirical data which was collected from the previously mentioned 5 approaches. Because the traffic signals on this road are all actuated depending on the real-time traffic, the offsets of this 5 approaches change with cycles. For being able to get more samples, all decimal offset numbers are turned into integers by the rounding-off method and extract modes for each approach. Then the cycles whose offsets are equal to the modes are observed and the corresponding SFRs are calculated. The HCM method is used to estimate the observed SFR, which is let 3600 divided by the average of the headways of all the vehicles in the queue except the first four vehicles, as the following equations show.

$$h_{si}=\frac{T_{ni}-T_{4i}}{n_i-4} \tag{14}$$

$$SFR_{obs}=\frac{3600}{h_{si}} \tag{15}$$

For approaches 1 and 4, their segment lengths are both 248m and cycles with 5s *offset* are analyzed. The downstream segment length of approach 2 is 218m and cycles with -13s *offset* is observed and calculated. The available data of approaches 3 and 5 is not enough for comparison thus they are not considered in this part. A total of 38 cycles are analyzed and the result of the comparison is shown in Fig. 11(a) and (b).

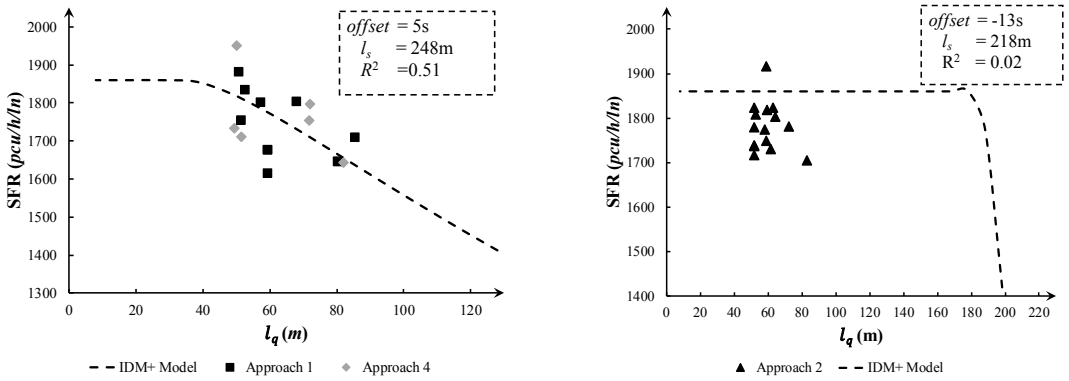

(a) Approach 1 and approach 4 (b) Approach 2

Fig. 11. Comparison with empirical data.

The data points of approach 1 and approach 4 are located in the downward phase of the curve and evenly distributed on both sides of the curve. Due to the positive offset value, the SFRs in the interval between l_q=50m and l_q=80m show a clear decreasing trend and the determinant coefficients R^2 is 0.51. Considering the randomness of driver's behavior, it can be called that the proposed model has a good fit to the empirical data under downstream influences.

While in Fig. 11(b) the data points of approach 2 are located near the flat part of the curve because of the low offset value and the short downstream queue length. However, most of them are distributed below the prediction curve, which leads to a low determinant coefficient (R^2=0.51). The following three reasons can account for this phenomenon: (1) randomness of driver's behavior; (2) the distance between its downstream intersection and the next 2nd intersection are very short, thus, behaviors of vehicles are affected by two intersections simultaneously as Fig. 12 shows; (3) the road segment connecting the downstream intersection and the next 2nd intersection has a 120-degree curve, drivers may slow down their speed because of the limited sight distance. The above three reasons do not belong to the downstream impact category of this study, so the differences in Fig. 11(b) are understandable.

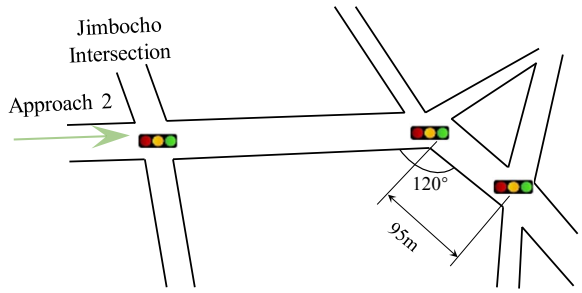

Fig. 12. Site description of approach 2

6. Conclusion

With the increase in traffic demand, the queue length in the downstream segment becomes longer resulting in a poor performance of upstream discharge flow. This phenomenon happens frequently in the urban area where intersections are closely spaced. In this paper, a new model was proposed based on improved IDM considering the downstream influence and it was calibrated with the genetic algorithm by using real trajectory data. During calibration, the relationship between the position in the upstream platoon and downstream impacts were discussed. It was revealed that the influence will decrease as the position moves behind and it will be an interesting topic in the future to study the relationship considering different geometric designs.

Through simulations, it was found that as the queue in the downstream segment becomes longer and the positive offset between the downstream intersection and upstream intersection become larger, the SFR at the upstream intersection approach tends to deteriorate. Also, the short downstream segment link will further intensify this effect. The above results are consistent with trends got from the empirical study, which means that the new model can reproduce real phenomena and be adopted to estimate the influenced SFR value.

By comparing with observed data, it was found that descending segments of the model curve fit the empirical data well. Whereas the stationary region of the model curve is obviously higher than observed data and the difference can be explained by complex effects of multiple factors. Most of the factors are outside the scope of this study which should be excluded. For further validation, more appropriate survey sites should be selected and investigated. In addition, it was found that upstream traffic flow could be further influenced by its secondary downstream intersection. The phenomenon implies that the downstream influence will gradually be transmitted along the upstream and it will be enlarged during the process. This topic is worth being discussed in the future.

Meanwhile, during the above analysis spillbacks are excluded. However, as an extreme case for downstream influence, it is meaningful to include all situations in one study. Thus, for the future research, the spillback influence should also be estimated by the new model. Furthermore, start-up lost time (SLT, hereinafter) and clearance lost time (CLT, hereinafter) also serve as important parameters in estimating the capacity and signal timing. An empirical study by Zhu and Nakamura (2018) revealed that queue length, available space, segment length, and offset play an important role in impacting SLT. With the downstream queue becomes longer, the SLT at the subject intersection tends to be higher. Therefore, it is necessary to continue to study how the new model can be adopted in estimating the SLT, CLT, and capacity considering downstream. The driver's optimization subconsciousness exist not only in the discharge processes at signalized intersections but also in all stages of travel, such as the deceleration behavior before approaching the congested area on the expressway. If in the future research, the proposed model can be further redesigned and be improved to be adapted to common travel process, the model will make more sense.

References

Highway Capacity Manual (HCM) 6th Edition, 2016. Transportation Research Board.

Rouphail, N.M., Akcelik, R., 1992. A Preliminary Model of Queue Interaction at Signalized Paired Intersections. Proceedings 16th Australian Road Research Board conference, Part 5.

Ahmed, K., Abu-Lebdeh, G., 2005. Modeling of Delay Induced by Downstream Traffic Disturbances at Signalized Intersections. Transportation Research Record: Journal of Transportation Research Board No. 1920, pp. 106-117.

The Traffic Signal Timing Manual, 2008. Federal Highway Administration (FHWA), U.S. Department of Transportation.

Hashemi, A. H., Nakamura, H., Goto, A., 2017. Influence of Downstream Conditions over Saturation Flow Rate, Proceedings of the 37th Conference of Japan Society of Traffic Engineers, pp. 467-472.

Yu, X., Sulijoadikusumo, G., 2012. Analysis of Downstream Queues on Upstream Capacity Expansion of Urban Signalized intersection, Journal of Transportation Systems Engineering and Information Technology Vol. 12, Issue 3, pp. 98-108.

Cohen, S., 2002. Application of car-following systems to queue discharge problem at signalized intersections, Transportation Research Record Journal of the Transportation Research Board 1802(1), pp. 205-213.

Treiber, M., Hennecke, A., Helbing, D., 2000. Congested traffic states in empirical observations and microscopic simulations. Phys Rev E Stat Phys Plasmas Fluids Relat Interdiscip Topics 62(2 Pt A), pp. 1805-1824.

Kesting, A., Treiber, M., 2008. Calibrating car-following models using trajectory data: methodological study. Transportation Research Record 2088, pp. 148-156.

Suzuki, K., Nakamura, H., 2006. Traffic Analyzer- the Integrated Video Image Processing system for Traffic Flow Analysis, Proceedings of the 13th World Congress on Intelligent Transportation Systems, London.

Zhu, H., Nakamura, H., 2018. Analysis on start-up lost time at closely spaced signalized intersections, Proceedings of Infrastructure Planning, No.57, 6 pages in CD-ROM.